



REVIEW

# Current approaches to studying membrane organization [version 1; referees: 3 approved]

**Thomas S. van Zanten, Satyajit Mayor**

National Centre for Biological Sciences (TIFR), Bellary Road, Bangalore, 560065, India

**v1** First published: 30 Nov 2015, 4(F1000 Faculty Rev):1380 (doi: 10.12688/f1000research.6868.1)

Latest published: 30 Nov 2015, 4(F1000 Faculty Rev):1380 (doi: 10.12688/f1000research.6868.1)

**Abstract**

The local structure and composition of the outer membrane of an animal cell are important factors in the control of many membrane processes and mechanisms. These include signaling, sorting, and exo- and endocytic processes that are occurring all the time in a living cell. Paradoxically, not only are the local structure and composition of the membrane matters of much debate and discussion, the mechanisms that govern its genesis remain highly controversial. Here, we discuss a swathe of new technological advances that may be applied to understand the local structure and composition of the membrane of a living cell from the molecular scale to the scale of the whole membrane.



This article is included in the [F1000 Faculty Reviews](#) channel.

**Open Peer Review****Referee Status:**

Invited Referees			
1	2	3	
version 1 published 30 Nov 2015			

F1000 Faculty Reviews are commissioned from members of the prestigious [F1000 Faculty](#). In order to make these reviews as comprehensive and accessible as possible, peer review takes place before publication; the referees are listed below, but their reports are not formally published.

**1** **Mary L Kraft**, University of Illinois at Urbana-Champaign USA

**2** **Paul W Wiseman**, McGill University Canada

**3** **Christian Eggeling**, University of Oxford UK

**Discuss this article**[Comments \(0\)](#)

**Corresponding authors:** Thomas S. van Zanten ([thomasvz@ncbs.res.in](mailto:thomasvz@ncbs.res.in)), Satyajit Mayor ([mayor@ncbs.res.in](mailto:mayor@ncbs.res.in))

**How to cite this article:** van Zanten TS and Mayor S. **Current approaches to studying membrane organization [version 1; referees: 3 approved]** *F1000Research* 2015, 4(F1000 Faculty Rev):1380 (doi: [10.12688/f1000research.6868.1](https://doi.org/10.12688/f1000research.6868.1))

**Copyright:** © 2015 van Zanten TS and Mayor S. This is an open access article distributed under the terms of the [Creative Commons Attribution Licence](#), which permits unrestricted use, distribution, and reproduction in any medium, provided the original work is properly cited.

**Grant information:** Thomas S. van Zanten acknowledges the European Molecular Biology Organization for a long-term fellowship (ALTF1519-2013). Satyajit Mayor thanks the Human Frontier Science Program (RGP0027/2012) for program support and the Department of Science and Technology (Government of India) for a JC Bose fellowship.

*The funders had no role in study design, data collection and analysis, decision to publish, or preparation of the manuscript.*

**Competing interests:** The authors declare that they have no competing interests.

**First published:** 30 Nov 2015, 4(F1000 Faculty Rev):1380 (doi: [10.12688/f1000research.6868.1](https://doi.org/10.12688/f1000research.6868.1))

## Introduction

“The stone age did not end because we ran out of stones”<sup>1</sup> ...

There has always been a close association between technological advancement and new research questions. A more recent example is how the application of x-ray crystallography to studying protein structures has opened up the possibility to elucidate structure and relate it to function<sup>2-4</sup>. In particular, how can single molecules transfer the genetic code into chemical and structural information? Research on the structure and organization of the cell membrane is undergoing a similar revolution with the application of (nano-) technological tools for the observation of membrane structure and composition.

The outer membrane of the living cell is the interface that demarcates the cell and its environment. Communication in either direction takes place largely via the local arrangement of proteins and lipids at the plasma membrane. Decades of research on the mobility and spatial organization of components in the membrane by fluorescence microscopy and electron microscopy (EM), respectively, have suggested that the membrane is structured as a fluid lipid bilayer<sup>5</sup>. More recent studies indicate that the membrane of the cell is not

a simple fluid where lipids form a well-behaved two-dimensional (2D) fluid and where proteins are solutes in this milieu. Instead, the plasma membrane is organized as a dynamic mosaic whose local assemblies can span nano- to mesoscopic scales<sup>6</sup> (Figure 1a).

It is important to understand how this organization, whether caused by thermodynamic fluctuations<sup>7</sup> or driven actively<sup>8,9</sup>, arises since it plays a significant role in the functioning of molecules embedded in this matrix. To build up a mechanistic understanding of how the cell effects this membrane organization, it is vital to have chemical, spatial, and temporal information of components in the cell membrane. Several technological advances are beginning to address these fundamental questions in more detail, and we will highlight how these are leading to a more complete picture of the cell membrane.

## High-resolution structural imaging

At the highest resolution, EM offers an unprecedented opportunity. With the development of cryo-EM tomography and of new detectors<sup>10</sup>, the possibilities of imaging molecular organization inside the cell are unparalleled. Macromolecular protein complexes of interest can be seen in the context of their natural environment with resolutions beyond the nanometer scale<sup>11-13</sup>. Contrast

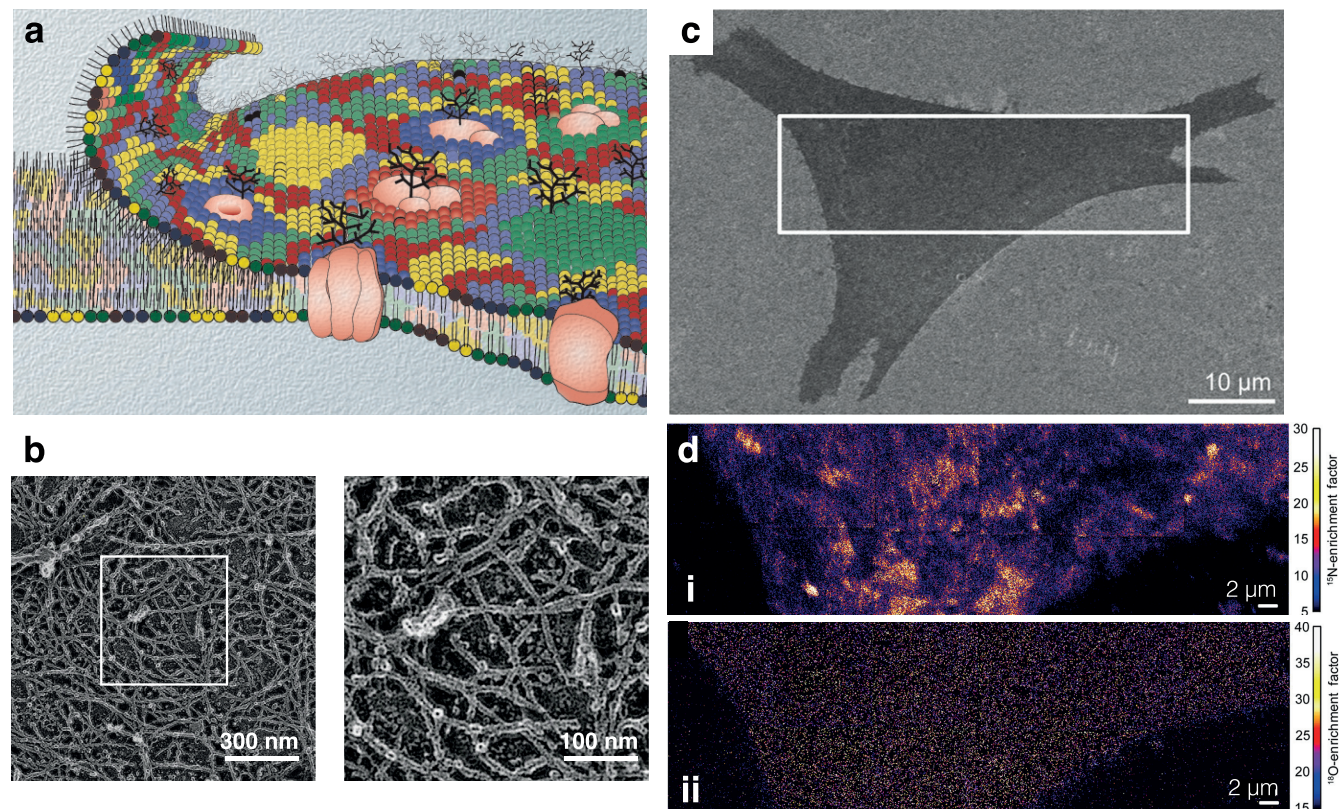


**Figure 1. A chemical view of the cell membrane.** (a) Image of membrane bilayer exhibits a patchwork mosaic of the distribution of lipids in the cell membrane and captures the lateral heterogeneity of the organization of membrane components in live cells. (b) This bilayer is anchored to the cortical actin meshwork as visualized by rapid-freeze deep-etch tomographic renderings of the cortical surface closest to the membrane. (c) Scanning electron microscopy image of a fibroblast cell. (d, i) The distribution of metabolically incorporated 15N-sphingolipids in the plasma membrane region indicated above represented as the detected sphingolipid-specific 15N-enrichment with NanoSIMS. Orange and yellow regions represent plasma membrane domains that are enriched with 15N-sphingolipids. (d, ii) The distribution of 18O-enrichment showing that the metabolically incorporated 18O-cholesterol is distributed relatively uniformly in the plasma membrane. Images (a), (b), and (c) and (d) are reproduced with permission from 6,19, and 35, respectively.

in EM, however, is chiefly dependent on electron density and has been directed to inquiries involving defined structures such as the cytoskeletal<sup>14,15</sup>, endocytic cups<sup>16,17</sup>, and adhesion plaques<sup>13,18</sup>. Noteworthy are several reports visualizing the interaction of the cortical actin with the membrane<sup>11,19</sup> where actin meshwork-like structures (Figure 1b), aside from providing mechanical stability and shape, could impede membrane protein diffusion<sup>19</sup>. The size and dynamics of these structures might well prove to be important for membrane-related reactions, priming specific cell function<sup>20,21</sup>. EM becomes especially powerful when combined with chemical specificity in the form of genetically tagged contrast agents<sup>22</sup> or through combination with fluorescence localization techniques<sup>23–25</sup>. However, obtaining chemically precise information with high resolution remains challenging.

### Chemically parsed spatial localization

The plasma membrane of any animal cell is composed of over 1,000 different types of lipids and proteins, presumably each with a specific purpose. Together, this assortment of chemical species at the plasma membrane primes the cell to adjust and react to the external milieu and communicate information about its internal state. Composition of both protein and lipid of the plasma membrane changes dramatically, depending on cell type<sup>26</sup>, developmental stage<sup>27</sup>, and pathological state<sup>28,29</sup>.

With the advent of sensitive mass spectrometry, it is now possible to construct a quantitative map of the entire protein and lipid composition of biochemically purified membranes<sup>30,31</sup>. The resulting *lipidome* or *proteome* of the membrane is evidence of the different sets of molecules that work together in space and time to perform function and process information. Access to their localization can be achieved (a) by label-free methods and (b) via high-contrast imaging of individual species.

### Label-free localization

Armed with a complete chemical composition of the membrane, obtaining the spatial organization of this information, preferably in real time and in a live cell, is the important next step. Matrix-assisted laser desorption ionization (MALDI) can locally vaporize material into ionized molecules or molecular fragments which are subsequently analyzed with a mass spectrometer. Raster-scanning the laser over a sample will generate an image with unprecedented chemical resolution, albeit at the rather low spatial scale of a few micrometers<sup>32</sup>.

At the expense of chemical bandwidth, magnetic sector secondary ion mass spectrometry (NanoSIMS) offers a typical spatial resolution of 100 nm on cell membranes<sup>33</sup>. In this method, a focused primary ion beam sputters neutral and ionized molecular fragments from the sample surface. These ejected secondary ions are subsequently collected and analyzed in the mass spectrometer. An additional benefit is a shallow sampling depth of 5 nm, which is due to the small secondary ion escape depth, making this technique exquisitely sensitive to the plasma membrane<sup>34</sup>. Because of the monoatomic and diatomic nature of the secondary ion component, identification is possible only if the molecules of interest contain distinct elements or isotopes<sup>33</sup>. For different lipids, this can be achieved by culturing cells in the presence of isotope-labeled precursors leading to their

metabolic incorporation into the lipid of interest, which would have the same chemical structure as its unlabeled analogue.

Chemical mapping of the plasma membrane displayed 200 nm domains showing a significant sphingolipid enrichment<sup>34</sup> (Figure 1c,d). These domains were further non-randomly assembled in patched regions that were about 3–10 μm in size<sup>34,35</sup>. Simultaneous chemical imaging of isotope-labeled cholesterol revealed that cholesterol, in contrast to sphingolipids, distributed in an apparent homogeneous fashion on the dorsal/upper membrane<sup>35</sup> analogously to a recent dynamic study<sup>36</sup>. Despite the non-overlapping spatial distribution, cholesterol depletion did disperse the sphingolipid-enriched domains. Actin depolymerization had a more dramatic effect, suggesting a link between lipid organization and the actin architecture<sup>35,37</sup>. With the possibility to include specific protein labeling along with the mapping of lipid components at the nanometer scale, this technique will continue to contribute to our understanding of the spatial distribution of chemistry in the membrane<sup>38,39</sup>.

The benefit of label-free methods is avoiding the possible influence of an attached label on the behavior of the specific protein or lipid of interest; for any lipid, given the mass ratio of a fluorescent label to the mass of the lipid species, this perturbation is likely to be substantial. Nevertheless, to get more detailed knowledge of how a cell constructs complexes in a membrane, molecular recognition with a high signal-to-noise ratio in an aqueous scattering milieu, a feature that label-free methods still lack, is essential.

### High-contrast imaging

Increase of signal-to-noise ratio is attained by specifically targeting or labeling the molecule of interest with, for example, an antibody, genetically, or by chemically incorporating a contrast agent. If the labels are carrying electron-dense material<sup>22</sup> or conjugated with gold nanoparticles<sup>40</sup>, they can be visualized with an electron microscope. In general, however, fluorescence light microscopy is used where individual targets of interest are coupled to fluorophores.

Focusing of light, however, is inherently diffraction-limited. With lens-based optics, light cannot be focused better than about 200–300 nm and individual objects that are spaced closer cannot be distinguished as unique objects anymore. To overcome this concentration limit<sup>41</sup>, several approaches have come up in the last decade to either (temporally) dilute the observed molecules (stochastic super-resolution microscopy<sup>42,43</sup>) or decrease the observation volume (targeted super-resolution microscopy<sup>44,45</sup>). Single-molecule imaging<sup>46</sup> has opened up a major avenue not only to observe the localization of single fluorophores at very high spatial resolution but also to study the biochemistry of individual species to derive ensemble properties of molecules inside a cell.

### Photo-localization microscopy

Optically interrogating the dynamic behavior of single molecules in their highly concentrated presence on the plasma membrane is made feasible by isolating a fluorescently labeled representative. Although the membrane components still move in their natural environment, their dynamics can now be characterized by recording the motion of a number of such ‘single representatives’ on a camera. If the distance between the individual molecules in each image

is larger than the diffraction limit, their positions can be determined with nanometer precision<sup>47,48</sup>. This accuracy of determining its center-of-mass is essentially inversely proportional to the square root of the number of photons emitted<sup>47</sup>. The positions of multiple fluorescent spots can be identified and related to their position in earlier images to build up their time trajectories<sup>49</sup>. The number of molecules can be tuned via the concentration of externally added specific markers, photo-activation of only a subset of fluorescent molecules<sup>50–52</sup>, or the photo-bleaching of a well-defined area followed by the sparse diffusion back in the observation area<sup>53,54</sup>. At the other end, technical advances in hyper-spectral detection should increase single-particle discrimination allowing an increase in concentrations of single molecular representatives<sup>55</sup>.

Recording a sufficient number of tracks or a single molecule for a sufficiently long time builds up the statistical behavior of the membrane components in terms of the diffusion coefficient or type of mobility<sup>56</sup>. Individual trajectories pooled into a distribution of diffusion coefficients can then be related to the functional/affinity state of a receptor<sup>57,58</sup>. Local changes in the individual trajectory can be mapped out on the cell to indicate the nature of the area traversed<sup>59,60</sup>, in terms of diffusion<sup>50</sup>, confinement regions<sup>61</sup>, or local energetic changes<sup>62</sup>. Examining the individual tracks of receptors as they diffuse in the plasma membrane revealed that they could become obstructed by lipid domains<sup>63</sup>, protein-protein interaction<sup>64</sup>, tetraspanin network<sup>65</sup>, glycan structures<sup>59,66</sup>, or the actin cytoskeleton<sup>57–69</sup> (Figure 2a,b).

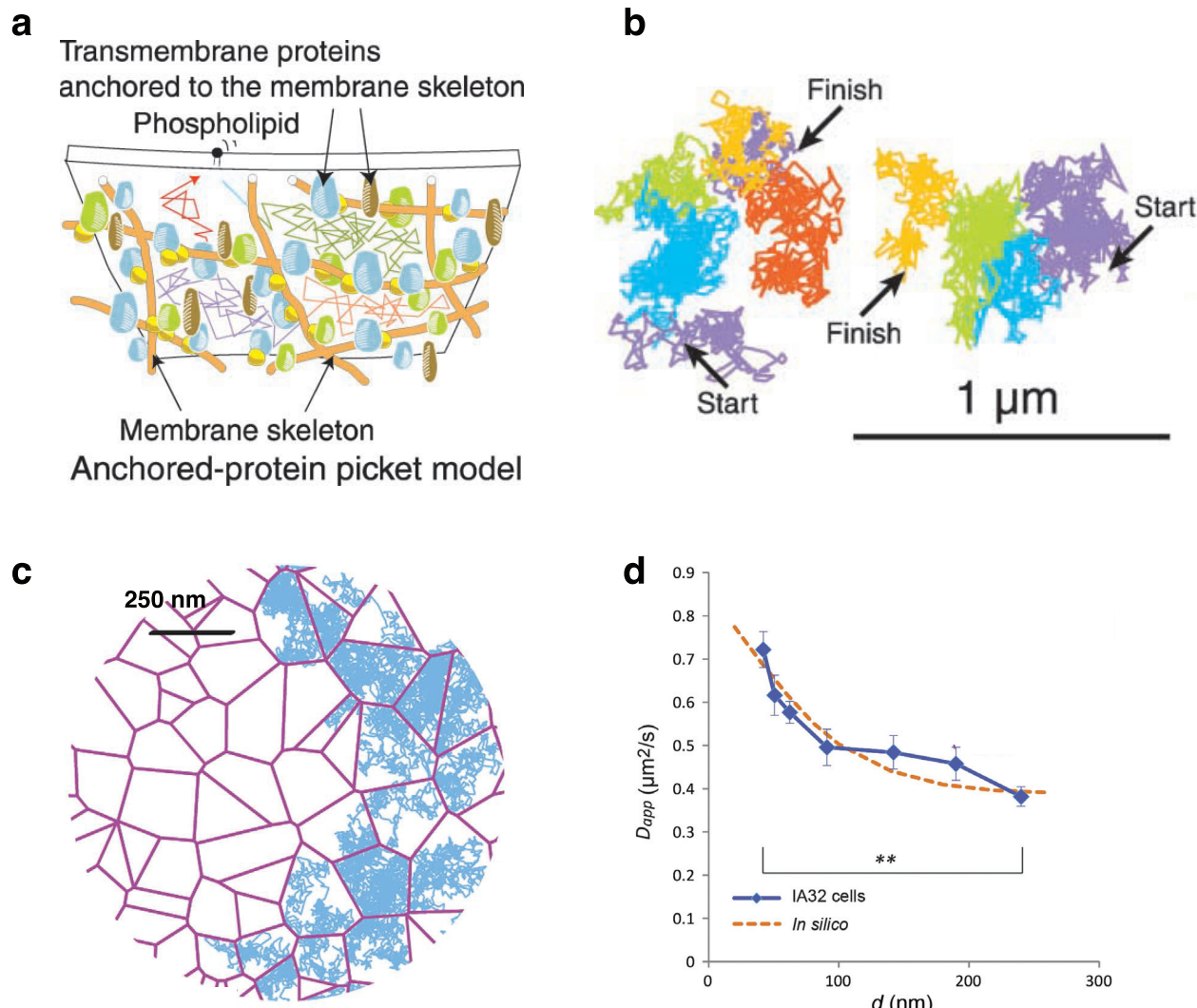


**Figure 2. A dynamic view of the membrane.** (a) Picket-fence model where transmembrane proteins anchored to the actin membrane skeleton meshwork effectively act as rows of pickets and temporarily confine the movement of lipids and proteins through steric hindrance and circumferential slowing (packing or frictional) effects. (b) Two representative trajectories of 1,2-dioleoyl-sn-glycero-3-phosphoethanolamine (DOPE) lipids on a living cell membrane recorded at a time resolution of 25  $\mu\text{s}$  (40,500 frames/s) for a period of 56 ms (2,250 frames) where plausible compartments are shown in different colors. (c) Schematic Voronoi lattices (purple) representative of actin-based compartment sizes together with simulated diffusion trajectories (cyan). Scale bar: 250 nm. (d) Dependency of the apparent diffusion coefficient of di-palmitoyl phosphoethanolamine (DPPE) lipids on the area of observation (blue line). Images reproduced with permission from 69 (a,b) and 135 (c,d).

Detection of changes due to interactions or confinement within boundaries of a compartment is reflected in changes in the molecular diffusion coefficient, which in turn depends on interaction strengths, acquisition speed, and signal-to-noise ratio (localization accuracy)<sup>70</sup>. On the other hand, prior information on molecular mobility could facilitate teasing out a subset of molecules without effectively diluting the experiment. If the subset (of interest) moves significantly slower because of an activation event or substrate binding, it is possible to experimentally deconvolve out the contribution of individual players in the reduction of mobility<sup>60,71</sup>. Using relatively long exposure/integration times, fast-moving fluorescent molecules blur into the background while slower moving molecules emit photons from the same diffraction-limited volume and therefore can be localized.

### Stochastic super-resolution microscopy

The stochastic cycling of dyes between fluorescent *on*-states and non-fluorescent *off*-states is an unfavorable property for single-molecule tracking because the single molecule might become undetectable in several frames and get lost during the trace reconstruction. Alternatively, if tuned properly, this cycling between states can be used to temporarily dilute highly concentrated samples. The challenge is to have at each given time only a subset of molecules in the *on*-state and determining the center-of-mass for each molecule before they switch *off* again. If this process is repeated many times, all of the calculated positions can be used to reconstruct a “super-resolution” image<sup>72</sup>. This indeed is the concept of the localization techniques called stochastic optical reconstruction microscopy (STORM)<sup>73</sup> and (fluorescent) photoactivatable localization microscopy, or (f)PALM<sup>42,43</sup>. Whereas STORM is essentially based on organic dyes that reversibly switch between *on*- and *off*-states<sup>74–77</sup>, PALM is based on engineered fluorescent proteins<sup>78–80</sup>.

Photo-localization-based super-resolution is excellent in determining sub-resolution complexes such as the endocytic clathrin-coated pits<sup>81,82</sup>, microtubular structures<sup>83–85</sup>, cytoskeletal structures<sup>86,87</sup>, and adhesion plaques<sup>88,89</sup> (Figure 3). Quantitative analysis of super-resolved domains in the plasma membrane in terms of absolute number of molecules is challenging because of blinking<sup>90</sup> and activation efficiency<sup>91</sup>. Nevertheless, analytical methods such as the pair-correlation<sup>92</sup> and Ripley’s K function<sup>93,94</sup> have allowed a certain degree of quantification, but this is strongly dependent on the assumptions employed in applying these statistical analyses to the data.

Since photo-localization-based super-resolution is based on a random spatial sampling of the structure, activating or switching light pulses are not necessarily required. In fact, it is possible to make use of the intrinsic trait of fluorophores to get temporarily trapped in a dark state, blinking. By engineering fluorophores that have longer dark states<sup>95</sup> or exploiting the known on-off blinking of quantum dots<sup>96</sup>, the chances that nearby emitters are both in an *on*-state decrease. On the other hand, one could tune incorporation rates of fluorescent species to the membrane (proteins); in a bath of freely diffusing fluorescent ligands, only the temporarily bound ligands will be detected, essentially taking advantage of mobility difference between bound and unbound<sup>97–99</sup>.

### Targeted super-resolution microscopy

Super-resolution imaging in the context of breaking Abbe’s diffraction limit has been achieved by decreasing the observation volume below the diffraction limit of light. This has been mainly accomplished with (a) use of near-field geometries or restricted physical apertures to confine the excitation volume or (b) the clever use of lasers to selectively deplete excited fluorophores in all except the very center of the optical volume to confine the emission volume.

**(a) Near-field optics.** By physically confining the light inside a very small aperture of 50–150 nm in diameter, light propagation is discontinued and the electromagnetic fields become restricted to the aperture (i.e., to the near field). The light intensity exponentially decays away from the aperture, producing essentially a nanoscopic excitation source. For imaging purposes, such a sub-wavelength aperture is created in a tapered aluminum-coated optical fiber. The image can then be built up by raster-scanning the aperture in close proximity to the sample and in fact this was one of the first approaches to obtain super-resolution images<sup>45</sup>. Because the rendering of the image is independent of the photo-physical properties of the sample/fluorophore, it allows near-field scanning optical microscopy (NSOM) to obtain quantitative information at the nanometer scale. Additionally, the same physical aperture confines multiple wavelengths and the technique is therefore free from chromatic aberrations<sup>100,101</sup>. Colocalization<sup>102</sup> among multiple chemical species (due to biochemical interaction), random scattering<sup>101</sup> (due to the lack of interaction), and segregation<sup>103</sup> are not the only modes of organization. Indeed, multicolor super-resolution imaging revealed multi-domain proximity on the order of 50–150 nm as another tendency<sup>101,104,105</sup>. Diffraction-limited techniques would erroneously identify such proximity as colocalization, showing the merit of any super-resolution technique. Proximity does not preclude interaction, and quantitative analysis showed that integrin activation could bias the glycosyl phosphatidylinositol-anchored protein (GPI-AP) organization to a more clustered state<sup>105</sup>. This more detailed quantification was granted by the possibility of having single-molecule sensitivity at the nanometer scale. Practical resolution of NSOM, however, is limited to approximately 50–70 nm, driving the field toward the use of optical antennas. Optical antennas, analogous to their radio frequency equivalent, convert freely propagating electromagnetic radiation into localized energy, and vice versa. Initial experiments have shown resolutions of 30–50 nm of proteins on a plasma membrane using a gold nano-particle<sup>106</sup> or a sculpted monopole<sup>107</sup> as photonic antenna. Recent advances in antenna design provided simultaneous multicolor localization accuracies well below 1 nm with low photon budgets<sup>108</sup>, showing tremendous potential for nanoscale sensing or imaging<sup>109</sup>. Near-field imaging or spectroscopy, however, is confined to sample surfaces that are accessible to the physical aperture/probes, making *in vivo* imaging inside cells a very difficult proposition.

**(b) Stimulated emission depletion.** A different strategy toward true super-resolution is to confine the emission instead of the excitation<sup>110</sup>. Its principle is based on the positionally deterministic switching of the fluorophore state in contrast to the stochastic switching for localization-based super-resolution<sup>111,112</sup>. Stimulated

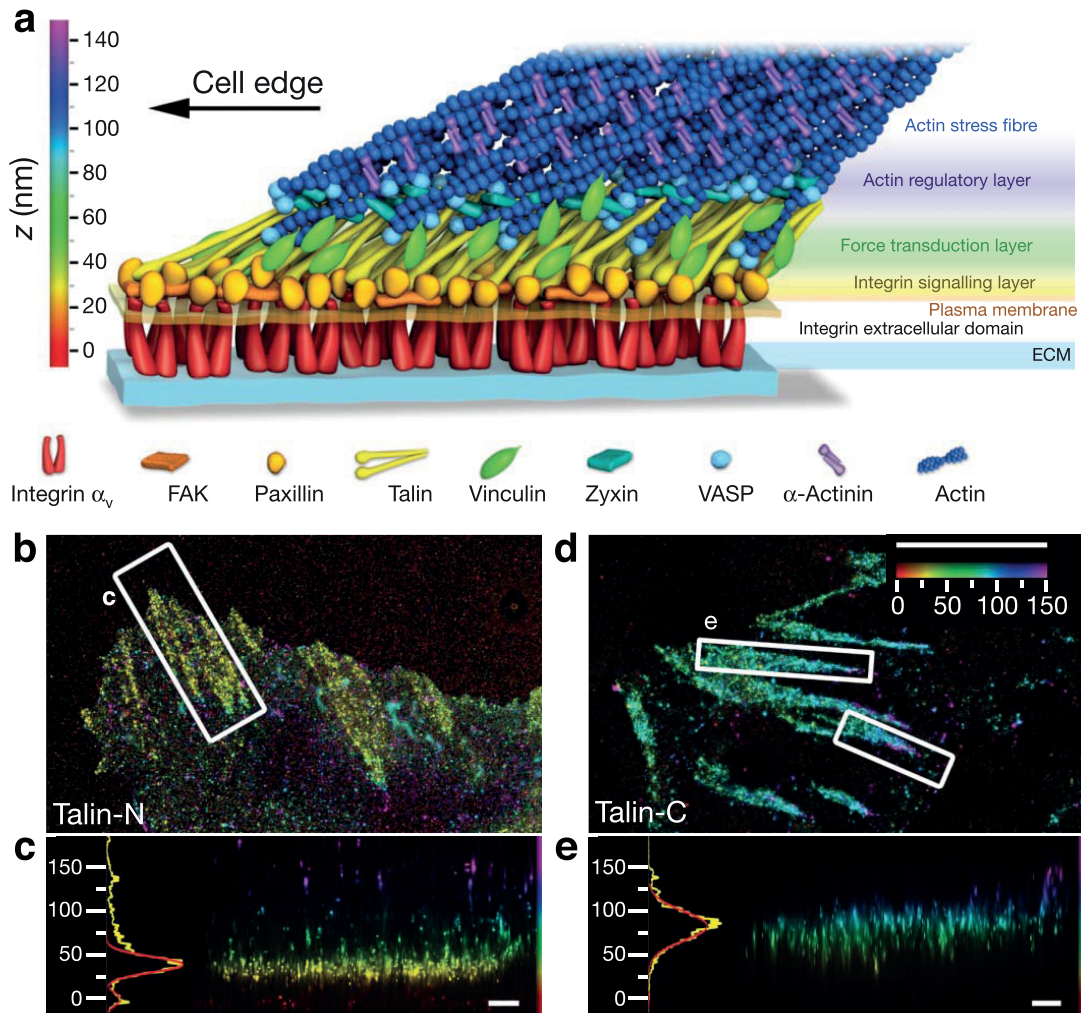


**Figure 3. A super-resolution view of membrane associated focal adhesions.** (a) Schematic model of the molecular architecture of focal adhesions. This model is based on the protein position measurement by interferometric photoactivatable localization microscopy (iPALM). The exquisite sensitivity of iPALM to register axial distances could determine the orientation of talin within focal adhesions. (b–e) Top and side views of iPALM images of focal adhesions (white boxes, top-view panels) and corresponding z histograms. Color encodes distance from the coverglass surface in nanometers. Placing the fluorescent probe at the two ends of the talin rod show that the N-terminus of talin rod localizes close to the cytoplasmic tails of integrin (b, c), whereas the C-terminus can localize up to 40 nm higher (d, e). Scale bars: 5 μm (b, d) and 500 nm (c, e). Images reproduced with permission from 89. Abbreviations: ECM, extracellular matrix.

emission depletion (STED) microscopy is founded on depleting the excited state of a fluorophore by stimulating the excited fluorophore to emit a photon of specified wavelength. By creating a highly intense donut-shaped emission depletion region around the confocal excitation volume, only the fluorophores in the center of the donut are spontaneously emitting in the detected wavelengths. By increasing the intensity of the depletion donut, the resolution of the microscope is increased. STED imaging has been used to identify and quantify cluster sizes in cell membranes<sup>59,113–115</sup>. The cluster sizes ranged from 50 to 160 nm, and STED experiments on membrane sheets indicated that the protein clusters were fine-tuned by electrostatic interactions and that these clusters are further assembled in relatively stable multi-protein assemblies<sup>116</sup>. Further development of the technique toward parallelization<sup>117,118</sup>, multicolor acquisition<sup>119–121</sup>,

and different illumination schemes<sup>122,123</sup> will definitely increase imaging capacity. Better spatial resolution, however, is accompanied by an increased *on-off* cycling load on the fluorophore during scanning, requiring further progress in fluorophore engineering.

#### Fluorescence fluctuation spectroscopy

Instead of demanding the heavy burden of photo stability from the fluorophore during multiple rounds of irradiation in the course of image build-up, one could allow the molecule itself to diffuse through the observation volume. During this passage, a fluorescent molecule will cause an intensity burst that is inversely proportional to the number of molecules in the observation volume. When sufficient numbers of molecules have passed, the detected intensity fluctuations can be autocorrelated, designating the technique as

fluorescence correlation spectroscopy (FCS). The time at which this autocorrelation function decays to half its original value corresponds to the characteristic timescale at which the molecules move through the observation volume.

There is a linear relationship between the diffusion time and the area of observation for 2D diffusion in the plasma membrane. The slope of this relation is inversely proportional to the apparent diffusion coefficient, and the time-axis intercept, obtained from extrapolation, is indicative of confinement<sup>124</sup>. According to this methodology, particles diffusing in the membrane can be divided in three major categories: (a) random diffusive, (b) domain interacting, and (c) meshwork constrained<sup>125,126</sup>. Exploitation of the FCS diffusion-law methodology found that sphingolipid- and cholesterol-dependent nanoscale domains are crucial for signaling<sup>127</sup>.

Similar methods of optically diluting the sample, as described above, can be employed for FCS<sup>128</sup>. More powerful is the combination of super-resolution techniques that confine the observation volume with FCS since this allows the registration of dynamics at the nanometer scale<sup>129–132</sup>. Mobility characteristics at the nanometer scale do not have to be extrapolated anymore<sup>125,126,133</sup> but can be directly measured<sup>130,134,135</sup> (Figure 2c,d). In fact, extensive research using the tunable nanoscopic observation volume provided by STED indicated that fast-moving lipid analogues exhibit distinct modes of mobility that can be divided in three classes<sup>130,136–139</sup>: (a) weak interactions of phosphoglycerolipids, (b) cholesterol-assisted binding mediated by the ceramide group, and (c) hydroxyl headgroup-assisted cholesterol-independent binding. In the future, bridging length scales with, for example, camera-based FCS<sup>140–142</sup> or spatio-temporal image correlation spectroscopy<sup>143–146</sup> should allow the visualization of how these fluctuating nanoscale assemblies can be stabilized to coalesce into functional signaling platforms<sup>7</sup>.

With the advent of reproducible nanofabrication techniques, a whole new field lies open for exploration. Engineered substrates can provide aperture-based<sup>134,147–150</sup> or optical antenna-based<sup>151,152</sup> nanofocusing of light on conventional microscopes. By virtue of the cells adhering to the substrate, the plasma membrane is brought in the near field of various nanoscopic excitation sources. Each of these excitation hotspots can now be addressed to locally probe membrane dynamics down to 20 nm<sup>152</sup> or in a multicolor fashion<sup>150</sup>.

### Measuring molecular interactions in the membrane

Multiple components in the cell membrane work together and interact to effectuate signaling. Interacting molecules would diffuse together through the excitation volume. Measuring the fluorescence cross-correlation in an FCS setup will therefore display a correlation proportional to the interaction between the two particles<sup>153,154</sup>. Cross-correlation analysis among probes with different membrane anchoring units suggested domain formation but reiterated the notion of a complex underlying machinery<sup>155</sup> that is not necessarily instructed by phase transitions<sup>156</sup>.

As an alternative to multi-particle tracking<sup>157</sup> and cross-correlation spectroscopy<sup>158</sup>, a more direct path to uncover nanoscale multimolecular mixing is Förster resonance energy transfer (FRET). Here, the energy of the excited state of a fluorophore (donor) is non-radiatively transferred to a neighboring fluorophore (acceptor). Upon returning to the ground state, the acceptor fluorophore subsequently emits a photon with different characteristics—lifetime<sup>159</sup>, polarization<sup>160</sup>, or Stokes-shifted<sup>161</sup>—as compared with an unperturbed donor fluorophore. Measurement of energy transfer between like fluorophores, *homo*-FRET, has been instrumental in the determination of small actively maintained nanoclusters<sup>8,162</sup> (Figure 4a). The constant fraction of dense nanoclusters at a large range of concentrations<sup>163–165</sup> together with large fluctuations in local density

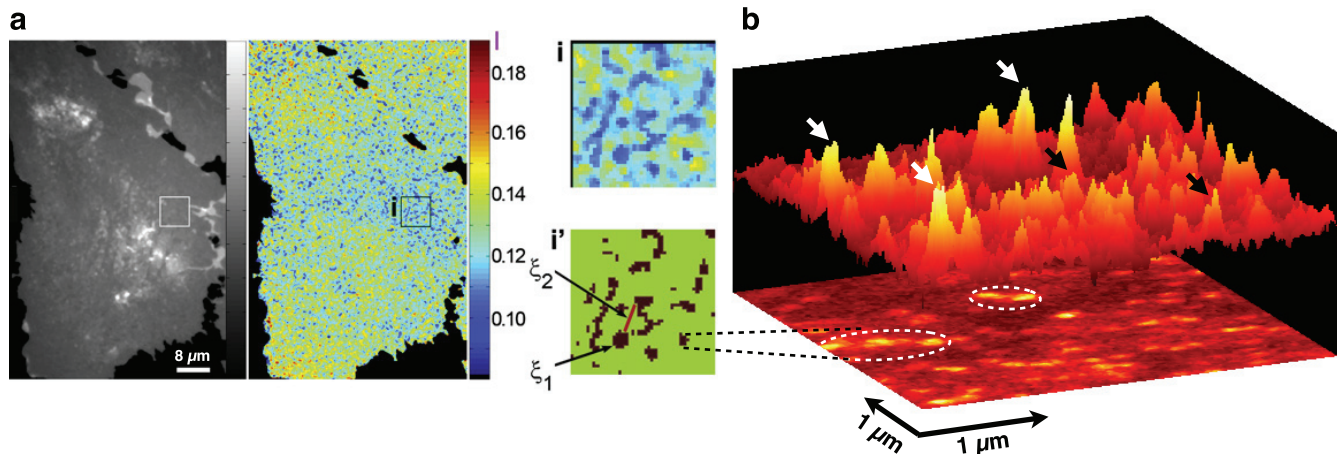


**Figure 4. A spatial view of the cell membrane: hierarchical organization of proteins.** (a) Quantitative analysis of the spatial distribution of glycosyl phosphatidylinositol-anchored proteins (GPI-APs). On flat regions of relatively constant fluorescence intensity (grayscale), the anisotropy images (pseudocolored, where low values indicate increased numbers of clusters) display a hierarchical distribution of GPI-AP (e.g., in the form of nanoclusters and characteristic distances between nanocluster-rich regions). *Homo*-Förster resonance energy transfer (*h*-FRET) imaging reports on the molecular proximity of like fluorophores at the 1- to 10-nm scale but imaging is still diffraction-limited and has no access to the region between 10 and 300 nm. (b) A super-resolution technique such as near-field scanning optical microscopy (NSOM) can provide access to these spatial scales and revealed GPI-AP nanoclusters to organize in 150- to 300-nm sized regions. Three-dimensional projection of a fluorescence intensity NSOM image with nanodomains (black arrows) and monomers (white arrows) of GPI-APs is shown. Contour dashed lines on the two-dimensional image illustrate the preference of nanodomains to concentrate on specific sites as hotspots. Images reproduced with permission from 165 (a) and 105 (b).

distribution<sup>165,166</sup> of lipid-anchored proteins is inconsistent with thermal equilibrium. Recognizing that a cortical layer of actin and myosins can drive membrane components by the consumption of energy is reconcilable with non-equilibrium membrane organization. The resolution of the FRET signal is intrinsically limited by the optical resolution; however, combining super-resolution methods as those described above with FRET opens up using the information of molecular proximity at the nanometer scale with structure and organization at the tens of nanometers offered, for example, by NSOM (Figure 4b).

In such a composite, intermolecular connections in the membrane are being complemented by the interactions of each component with the underlying cortical actin<sup>9</sup>. Although *inert* particles are not influenced by the cortical actin<sup>165,166</sup>, interactions of *passive* particles to the actin can be either direct<sup>166</sup> or indirect<sup>167</sup>. The formations of these local domains can subsequently be used as a signaling platform<sup>127,157,168</sup>. At the same time, the acto-myosin-dependent localization of domain creation and dissipation allows the cell to tune information-processing capacities of *passive* particles<sup>20,169</sup>. In this context, one can define a third class of membrane components as *active*: the membrane particles preoccupied with the tuning process. Examples of this last category are integrins<sup>170,171</sup>, G protein-coupled receptors<sup>172</sup>, and T-cell receptors<sup>173,174</sup>, all of which are intricately involved in cortical actin reshaping.

## Outlook on disentangling molecular function

Precise positional information of proteins, even in the context of their chemical and topographical environment, might not always be enough to tease out how a particular mechanism works. New tools such as sensors that can identify activation state will help elucidating the spatial patterns behind activating signals<sup>175–178</sup>. On the other hand, one could effectively influence the system via substrate-controlled calibration<sup>179</sup>, recruitment<sup>180,181</sup>, or perturbations<sup>182,183</sup> and optogenetic regulation of protein (de)activation<sup>184–187</sup>. A completely different but nevertheless informative approach would be an *in vitro* assay to help untangle a mechanistic understanding of cellular behavior<sup>188–193</sup>. By taking the process out of the cell, one can rebuild step-by-step and investigate the minimal chemistry required to regain function<sup>194</sup>.

A growing myriad and fruitful blend of interdisciplinary methodologies and technical improvements are shedding light on the spatio-temporal fluctuations of functional chemistry that underlies cellular behavior. This is captured in a 2D plot that maps the landscape of these possibilities (Figure 5). Of note is the observation that a large fraction of the area of this map is occupied, and only a few regions remain unpopulated by methods available today. It is only a matter of time until we can directly follow the evolution of nanoscale heterogeneities to microscale patterning of plasma membrane components after receptor activation.

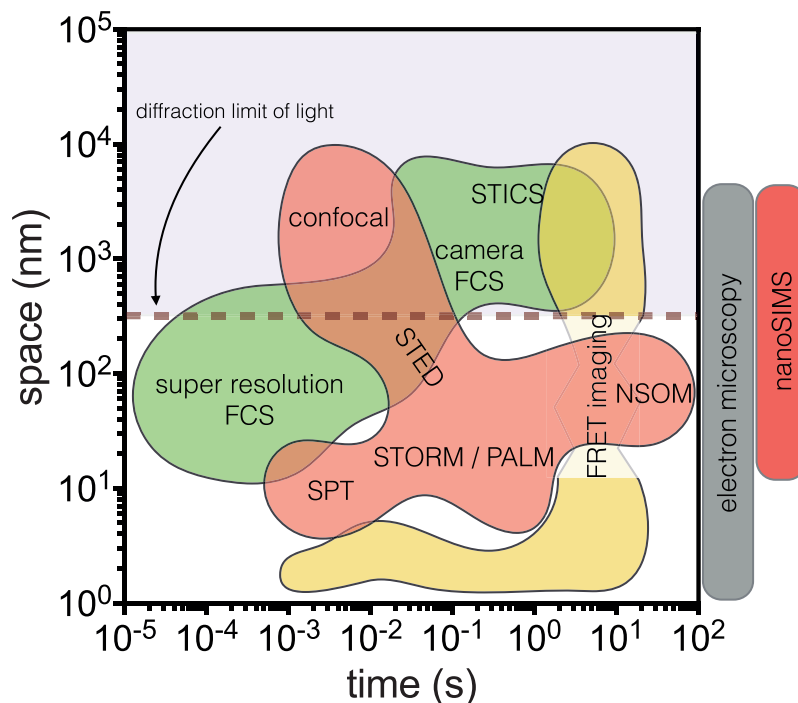


**Figure 5. Space and time resolution of current methods.** Representation of the landscape that current methods occupy in the space and time axes. Abbreviations: FCS, fluorescence correlation spectroscopy; FRET, Förster resonance energy transfer; NSOM, near-field scanning optical microscopy; PALM, photoactivatable localization microscopy; SPT, single particle tracking; STED, stimulated emission depletion; STICS, spatio-temporal image correlation spectroscopy; STORM, stochastic optical reconstruction microscopy.

## Abbreviations

2D, two-dimensional; EM, electron microscopy; FCS, fluorescence correlation spectroscopy; FRET, Förster resonance energy transfer; NSOM, near-field scanning optical microscopy; PALM, photoactivatable localization microscopy; STED, stimulated emission depletion; STORM, stochastic optical reconstruction microscopy.

## Competing interests

The authors declare that they have no competing interests.

## Grant information

Thomas S. van Zanten acknowledges the European Molecular Biology Organization for a long-term fellowship (ALTF1519-2013). Satyajit Mayor thanks the Human Frontier Science Program (RGP0027/2012) for program support and the Department of Science and Technology (Government of India) for a JC Bose fellowship.

*I confirm that the funders had no role in study design, data collection and analysis, decision to publish, or preparation of the manuscript.*

## References

1. Quote originally attributed to former Saudi oil minister. Sheik Ahmed Zaki Yamani ca 1970s.
2.  Wlodawer A, Minor W, Dauter Z, et al.: Protein crystallography for non-crystallographers, or how to get the best (but not more) from published macromolecular structures. *FEBS J.* 2008; 275(1): 1–21.  
[PubMed Abstract](#) | [Publisher Full Text](#) | [Free Full Text](#) | [F1000 Recommendation](#)
3. Carpenter EP, Beis K, Cameron AD, et al.: Overcoming the challenges of membrane protein crystallography. *Curr Opin Struct Biol.* 2008; 18(5): 581–6.  
[PubMed Abstract](#) | [Publisher Full Text](#) | [Free Full Text](#)
4. Wlodawer A, Minor W, Dauter Z, et al.: Protein crystallography for aspiring crystallographers or how to avoid pitfalls and traps in macromolecular structure determination. *FEBS J.* 2013; 280(22): 5705–36.  
[PubMed Abstract](#) | [Publisher Full Text](#) | [Free Full Text](#)
5. Singer SJ, Nicolson GL: The fluid mosaic model of the structure of cell membranes. *Science.* 1972; 175(4023): 720–31.  
[PubMed Abstract](#) | [Publisher Full Text](#)
6. Edidin M: The state of lipid rafts: from model membranes to cells. *Annu Rev Biophys Biomol Struct.* 2003; 32: 257–83.  
[PubMed Abstract](#) | [Publisher Full Text](#)
7.  Lingwood D, Simons K: Lipid rafts as a membrane-organizing principle. *Science.* 2010; 327(5961): 46–50.  
[PubMed Abstract](#) | [Publisher Full Text](#) | [F1000 Recommendation](#)
8. Mayor S, Rao M: Rafts: scale-dependent, active lipid organization at the cell surface. *Traffic.* 2004; 5(4): 231–40.  
[PubMed Abstract](#) | [Publisher Full Text](#)
9. Rao M, Mayor S: Active organization of membrane constituents in living cells. *Curr Opin Cell Biol.* 2014; 29: 126–32.  
[PubMed Abstract](#) | [Publisher Full Text](#)
10. Faruqi AR, Henderson R: Electronic detectors for electron microscopy. *Curr Opin Struct Biol.* 2007; 17(5): 549–55.  
[PubMed Abstract](#) | [Publisher Full Text](#)
11.  Medalia O, Weber I, Frangakis AS, et al.: Macromolecular architecture in eukaryotic cells visualized by cryoelectron tomography. *Science.* 2002; 298(5596): 1209–13.  
[PubMed Abstract](#) | [Publisher Full Text](#) | [F1000 Recommendation](#)
12.  Asano S, Fukuda Y, Beck F, et al.: Proteasomes. A molecular census of 26 proteasomes in intact neurons. *Science.* 2015; 347(6220): 439–42.  
[PubMed Abstract](#) | [Publisher Full Text](#) | [F1000 Recommendation](#)
13.  Patila I, Volberg T, Elad N, et al.: Dissecting the molecular architecture of integrin adhesion sites by cryo-electron tomography. *Nat Cell Biol.* 2010; 12(9): 909–15.  
[PubMed Abstract](#) | [Publisher Full Text](#) | [F1000 Recommendation](#)
14. Svitkina TM, Borisy GG: Arp2/3 complex and actin depolymerizing factor/cofilin in dendritic organization and treadmilling of actin filament array in lamellipodia. *J Cell Biol.* 1999; 145(5): 1009–26.  
[PubMed Abstract](#) | [Publisher Full Text](#) | [Free Full Text](#)
15. Jasmin M, Asano S, Gouin E, et al.: Three-dimensional architecture of actin filaments in *Listeria monocytogenes* comet tails. *Proc Natl Acad Sci U S A.* 2013; 110(51): 20521–6.  
[PubMed Abstract](#) | [Publisher Full Text](#) | [Free Full Text](#)
16. Sanan DA, Anderson RG: Simultaneous visualization of LDL receptor distribution and clathrin lattices on membranes torn from the upper surface of cultured cells. *J Histochem Cytochem.* 1991; 39(8): 1017–24.  
[PubMed Abstract](#) | [Publisher Full Text](#)
17.  Kirkham M, Fujita A, Chadda R, et al.: Ultrastructural identification of uncoated caveolin-independent early endocytic vehicles. *J Cell Biol.* 2005; 168(3): 465–76.  
[PubMed Abstract](#) | [Publisher Full Text](#) | [Free Full Text](#) | [F1000 Recommendation](#)
18. Luxenburg C, Geblinger D, Klein E, et al.: The architecture of the adhesive apparatus of cultured osteoclasts: from podosome formation to sealing zone assembly. *PLoS One.* 2007; 2(1): e179.  
[PubMed Abstract](#) | [Publisher Full Text](#) | [Free Full Text](#)
19.  Morone N, Fujiwara T, Murase K, et al.: Three-dimensional reconstruction of the membrane skeleton at the plasma membrane interface by electron tomography. *J Cell Biol.* 2006; 174(6): 851–62.  
[PubMed Abstract](#) | [Publisher Full Text](#) | [Free Full Text](#) | [F1000 Recommendation](#)
20. Chaudhuri A, Bhattacharya B, Gowrishankar K, et al.: Spatiotemporal regulation of chemical reactions by active cytoskeletal remodeling. *Proc Natl Acad Sci U S A.* 2011; 108(36): 14825–30.  
[PubMed Abstract](#) | [Publisher Full Text](#) | [Free Full Text](#)
21. Mugler A, Tostevin F, Wolde ten PR: Spatial partitioning improves the reliability of biochemical signaling. *Proc Natl Acad Sci U S A.* 2013; 110(15): 5927–32.  
[PubMed Abstract](#) | [Publisher Full Text](#) | [Free Full Text](#)
22.  Shu X, Lev-Ram V, Deerinck TJ, et al.: A genetically encoded tag for correlated light and electron microscopy of intact cells, tissues, and organisms. *PLoS Biol.* 2011; 9(4): e1001041.  
[PubMed Abstract](#) | [Publisher Full Text](#) | [Free Full Text](#) | [F1000 Recommendation](#)
23.  Kukulski W, Schorb M, Welsch S, et al.: Correlated fluorescence and 3D electron microscopy with high sensitivity and spatial precision. *J Cell Biol.* 2011; 192(1): 111–9.  
[PubMed Abstract](#) | [Publisher Full Text](#) | [Free Full Text](#) | [F1000 Recommendation](#)
24.  Kukulski W, Schorb M, Kaksonen M, et al.: Plasma membrane reshaping during endocytosis is revealed by time-resolved electron tomography. *Cell.* 2012; 150(3): 508–20.  
[PubMed Abstract](#) | [Publisher Full Text](#) | [F1000 Recommendation](#)
25.  Sochacki KA, Shtengel G, van Engelenburg SB, et al.: Correlative super-resolution fluorescence and metal-replica transmission electron microscopy. *Nat Methods.* 2014; 11(3): 305–8.  
[PubMed Abstract](#) | [Publisher Full Text](#) | [Free Full Text](#) | [F1000 Recommendation](#)
26. Sampiao JL, Gerl MJ, Klose C, et al.: Membrane lipidome of an epithelial cell line. *Proc Natl Acad Sci U S A.* 2011; 108(5): 1903–7.  
[PubMed Abstract](#) | [Publisher Full Text](#) | [Free Full Text](#)
27. Guan XL, Cestra G, Shui G, et al.: Biochemical membrane lipidomics during *Drosophila* development. *Dev Cell.* 2013; 24(1): 98–111.  
[PubMed Abstract](#) | [Publisher Full Text](#)
28. Zhang Z, Zhang L, Hua Y, et al.: Comparative proteomic analysis of plasma membrane proteins between human osteosarcoma and normal osteoblastic cell lines. *BMC Cancer.* 2010; 10(1): 206–9.  
[PubMed Abstract](#) | [Publisher Full Text](#) | [Free Full Text](#)
29. Ziegler YS, Moresco JJ, Tu PG, et al.: Plasma membrane proteomics of human breast cancer cell lines identifies potential targets for breast cancer diagnosis and treatment. *PLoS One.* 2014; 9(7): e102341–18.  
[PubMed Abstract](#) | [Publisher Full Text](#) | [Free Full Text](#)
30. Shevchenko A, Simons K: Lipidomics: coming to grips with lipid diversity. *Nat Rev Mol Cell Biol.* 2010; 11(8): 593–8.  
[PubMed Abstract](#) | [Publisher Full Text](#)
31. Cordwell SJ, Thingholm TE: Technologies for plasma membrane proteomics. *Proteomics.* 2010; 10(4): 611–27.  
[PubMed Abstract](#) | [Publisher Full Text](#)



32. Chaurand P, Cornett DS, Angel PM, et al.: From whole-body sections down to cellular level, multiscale imaging of phospholipids by MALDI mass spectrometry. *Mol Cell Proteomics*. 2011; 10(2): 1–11.  
[PubMed Abstract](#) | [Publisher Full Text](#) | [Free Full Text](#)
33. Kraft ML, Klitzing HA: Imaging lipids with secondary ion mass spectrometry. *Biochim Biophys Acta*. 2014; 1841(8): 1108–19.  
[PubMed Abstract](#) | [Publisher Full Text](#)
34. Frisz JF, Lou K, Klitzing HA, et al.: Direct chemical evidence for sphingolipid domains in the plasma membranes of fibroblasts. *Proc Natl Acad Sci U S A*. 2013; 110(8): E613–22.  
[PubMed Abstract](#) | [Publisher Full Text](#) | [Free Full Text](#) | [F1000 Recommendation](#)
35. Frisz JF, Klitzing HA, Lou K, et al.: Sphingolipid domains in the plasma membranes of fibroblasts are not enriched with cholesterol. *J Biol Chem*. 2013; 288(23): 16855–61.  
[PubMed Abstract](#) | [Publisher Full Text](#) | [Free Full Text](#)
36. Hiramoto-Yamaki N, Tanaka KA, Suzuki KG, et al.: Ultrafast diffusion of a fluorescent cholesterol analog in compartmentalized plasma membranes. *Traffic*. 2014; 15(6): 583–612.  
[PubMed Abstract](#) | [Publisher Full Text](#) | [Free Full Text](#)
37. Fujita A, Cheng J, Fujimoto T: Segregation of GM1 and GM3 clusters in the cell membrane depends on the intact actin cytoskeleton. *Biochim Biophys Acta*. 2009; 1791(5): 388–96.  
[PubMed Abstract](#) | [Publisher Full Text](#)
38. Wilson RL, Frisz JF, Hanafin WP, et al.: Fluorinated colloidal gold immunolabels for imaging select proteins in parallel with lipids using high-resolution secondary ion mass spectrometry. *Bioconjug Chem*. 2012; 23(3): 450–60.  
[PubMed Abstract](#) | [Publisher Full Text](#) | [Free Full Text](#)
39. Wilson RL, Frisz JF, Klitzing HA, et al.: Hemagglutinin clusters in the plasma membrane are not enriched with cholesterol and sphingolipids. *Biophys J*. 2015; 108(7): 1652–9.  
[PubMed Abstract](#) | [Publisher Full Text](#) | [Free Full Text](#) | [F1000 Recommendation](#)
40. Slot JW, Geuze HJ: Cryosectioning and immunolabeling. *Nat Protoc*. 2007; 2(10): 2480–91.  
[PubMed Abstract](#) | [Publisher Full Text](#)
41. Holzmeister P, Acuna GP, Grohmann D, et al.: Breaking the concentration limit of optical single-molecule detection. *Chem Soc Rev*. 2014; 43(4): 1014–28.  
[PubMed Abstract](#) | [Publisher Full Text](#)
42. Betzig E, Patterson GH, Sougrat R, et al.: Imaging intracellular fluorescent proteins at nanometer resolution. *Science*. 2006; 313(5793): 1642–5.  
[PubMed Abstract](#) | [Publisher Full Text](#) | [F1000 Recommendation](#)
43. Hess ST, Girirajan TP, Mason MD: Ultra-high resolution imaging by fluorescence photoactivation localization microscopy. *Biophys J*. 2006; 91(11): 4258–72.  
[PubMed Abstract](#) | [Publisher Full Text](#) | [Free Full Text](#)
44. Klar TA, Jakobs S, Dyba M, et al.: Fluorescence microscopy with diffraction resolution barrier broken by stimulated emission. *Proc Natl Acad Sci U S A*. 2000; 97(15): 8206–10.  
[PubMed Abstract](#) | [Publisher Full Text](#) | [Free Full Text](#)
45. Betzig E, Trautman JK, Harris TD, et al.: Breaking the diffraction barrier: optical microscopy on a nanometric scale. *Science*. 1991; 251(5000): 1468–70.  
[PubMed Abstract](#) | [Publisher Full Text](#)
46. Moerner WE, Kador L: Optical detection and spectroscopy of single molecules in a solid. *Phys Rev Lett*. 1989; 62(21): 2535–8.  
[PubMed Abstract](#) | [Publisher Full Text](#)
47. Thompson RE, Larson DR, Webb WW: Precise nanometer localization analysis for individual fluorescent probes. *Biophys J*. 2002; 82(5): 2775–83.  
[PubMed Abstract](#) | [Publisher Full Text](#) | [Free Full Text](#)
48. Yildiz A, Forkey JN, McKinney SA, et al.: Myosin V walks hand-over-hand: Single fluorophore imaging with 1.5-nm localization. *Science*. 2003; 300(5628): 2061–5.  
[PubMed Abstract](#) | [Publisher Full Text](#) | [F1000 Recommendation](#)
49. Chenuard N, Smal I, de Chaumont F, et al.: Objective comparison of particle tracking methods. *Nat Methods*. 2014; 11(3): 281–9.  
[PubMed Abstract](#) | [Publisher Full Text](#) | [Free Full Text](#)
50. Manley S, Gillette JM, Patterson GH, et al.: High-density mapping of single-molecule trajectories with photoactivated localization microscopy. *Nat Methods*. 2008; 5(2): 155–7.  
[PubMed Abstract](#) | [Publisher Full Text](#) | [F1000 Recommendation](#)
51. Benke A, Olivier N, Gunzenhäuser J, et al.: Multicolor single molecule tracking of stochastically active synthetic dyes. *Nano Lett*. 2012; 12(5): 2619–24.  
[PubMed Abstract](#) | [Publisher Full Text](#)
52. Rossier OM, Octeau V, Sibarita JB, et al.: Integrins  $\beta_1$  and  $\beta_3$  exhibit distinct dynamic nanoscale organizations inside focal adhesions. *Nat Cell Biol*. 2012; 14(10): 1057–67.  
[PubMed Abstract](#) | [Publisher Full Text](#) | [F1000 Recommendation](#)
53. Moertelmaier M, Brameshuber M, Linimeier M, et al.: Thinning out clusters while conserving stoichiometry of labeling. *Appl Phys Lett*. 2005; 87(26): 263903–4.  
[Publisher Full Text](#)
54. Brameshuber M, Weghuber J, Ruprecht V, et al.: Imaging of mobile long-lived nanoplates in the live cell plasma membrane. *J Biol Chem*. 2010; 285(53): 41765–71.  
[PubMed Abstract](#) | [Publisher Full Text](#) | [Free Full Text](#)
55. Cutler PJ, Malik MD, Liu S, et al.: Multi-color quantum dot tracking using a high-speed hyperspectral line-scanning microscope. *PLoS One*. 2013; 8(5): e64320–14.  
[PubMed Abstract](#) | [Publisher Full Text](#) | [Free Full Text](#)
56. Saxton MJ, Jacobson K: Single-particle tracking: applications to membrane dynamics. *Annu Rev Biophys Biomol Struct*. 1997; 26: 373–99.  
[PubMed Abstract](#) | [Publisher Full Text](#)
57. Cairo CW, Mirchev R, Golan DE: Cytoskeletal regulation couples LFA-1 conformational changes to receptor lateral mobility and clustering. *Immunity*. 2006; 25(2): 297–308.  
[PubMed Abstract](#) | [Publisher Full Text](#)
58. Bakker GJ, Eich C, Torreno-Pina JA, et al.: Lateral mobility of individual integrin nanoclusters orchestrates the onset for leukocyte adhesion. *Proc Natl Acad Sci U S A*. 2012; 109(13): 4869–74.  
[PubMed Abstract](#) | [Publisher Full Text](#) | [Free Full Text](#)
59. Torreno-Pina JA, Castro BM, Manzo C, et al.: Enhanced receptor-clathrin interactions induced by N-glycan-mediated membrane micropatterning. *Proc Natl Acad Sci U S A*. 2014; 111(30): 11037–42.  
[PubMed Abstract](#) | [Publisher Full Text](#) | [Free Full Text](#) | [F1000 Recommendation](#)
60. Das S, Yin T, Yang Q, et al.: Single-molecule tracking of small GTPase Rac1 uncovers spatial regulation of membrane translocation and mechanism for polarized signaling. *Proc Natl Acad Sci U S A*. 2015; 112(3): E267–76.  
[PubMed Abstract](#) | [Publisher Full Text](#) | [Free Full Text](#) | [F1000 Recommendation](#)
61. Sergé A, Bertaux N, Rigneault H, et al.: Dynamic multiple-target tracing to probe spatiotemporal cartography of cell membranes. *Nat Methods*. 2008; 5(8): 687–94.  
[PubMed Abstract](#) | [Publisher Full Text](#)
62. Masson JB, Dionne P, Salvatico C, et al.: Mapping the energy and diffusion landscapes of membrane proteins at the cell surface using high-density single-molecule imaging and bayesian inference: application to the multiscale dynamics of glycine receptors in the neuronal membrane. *Biophys J*. 2014; 106(1): 74–83.  
[PubMed Abstract](#) | [Publisher Full Text](#) | [Free Full Text](#)
63. Pinaud F, Michalet X, Iyer G, et al.: Dynamic partitioning of a glycosyl-phosphatidylinositol-anchored protein in glycosphingolipid-rich microdomains imaged by single-quantum dot tracking. *Traffic*. 2009; 10(6): 691–712.  
[PubMed Abstract](#) | [Publisher Full Text](#) | [Free Full Text](#)
64. Douglass AD, Vale RD: Single-molecule microscopy reveals plasma membrane microdomains created by protein-protein networks that exclude or trap signaling molecules in T cells. *Cell*. 2005; 121(6): 937–50.  
[PubMed Abstract](#) | [Publisher Full Text](#) | [Free Full Text](#) | [F1000 Recommendation](#)
65. Espenel C, Margeat E, Dosset P, et al.: Single-molecule analysis of CD9 dynamics and partitioning reveals multiple modes of interaction in the tetraspanin web. *J Cell Biol*. 2008; 182(4): 765–76.  
[PubMed Abstract](#) | [Publisher Full Text](#) | [Free Full Text](#) | [F1000 Recommendation](#)
66. Paszek MJ, DuFort CC, Rossier O, et al.: The cancer glycocalyx mechanically primes integrin-mediated growth and survival. *Nature*. 2014; 511(7509): 319–25.  
[PubMed Abstract](#) | [Publisher Full Text](#) | [Free Full Text](#)
67. Sako Y, Kusumi A: Compartmentalized structure of the plasma membrane for receptor movements as revealed by a nanometer-level motion analysis. *J Cell Biol*. 1994; 125(6): 1251–64.  
[PubMed Abstract](#) | [Publisher Full Text](#) | [Free Full Text](#)
68. Andrews NL, Lidek KA, Pfeiffer JR, et al.: Actin restricts FcepsilonRI diffusion and facilitates antigen-induced receptor immobilization. *Nat Cell Biol*. 2008; 10(8): 955–63.  
[PubMed Abstract](#) | [Publisher Full Text](#) | [Free Full Text](#)
69. Fujiwara T, Ritchie K, Murakoshi H, et al.: Phospholipids undergo hop diffusion in compartmentalized cell membrane. *J Cell Biol*. 2002; 157(6): 1071–81.  
[PubMed Abstract](#) | [Publisher Full Text](#) | [Free Full Text](#) | [F1000 Recommendation](#)
70. Ritchie K, Shan XY, Kondo J, et al.: Detection of non-Brownian diffusion in the cell membrane in single molecule tracking. *Biophys J*. 2005; 88(3): 2266–77.  
[PubMed Abstract](#) | [Publisher Full Text](#) | [Free Full Text](#)
71. O'Donoghue GP, Pielaik RM, Smilgoverts AA, et al.: Direct single molecule measurement of TCR triggering by agonist pMHC in living primary T cells. *eLife*. 2013; 2: e00778–8.  
[PubMed Abstract](#) | [Publisher Full Text](#) | [Free Full Text](#)
72. Sage D, Kirshner H, Pengo T, et al.: Quantitative evaluation of software packages for single-molecule localization microscopy. *Nat Methods*. 2015; 12(6): 717–24.  
[PubMed Abstract](#) | [Publisher Full Text](#)
73. Rust MJ, Bates M, Zhuang X: Sub-diffraction-limit imaging by stochastic optical reconstruction microscopy (STORM). *Nat Methods*. 2006; 3(10): 793–5.  
[PubMed Abstract](#) | [Publisher Full Text](#) | [Free Full Text](#) | [F1000 Recommendation](#)
74. Heilemann M, Margeat E, Kasper R, et al.: Carbocyanine dyes as efficient reversible single-molecule optical switch. *J Am Chem Soc*. 2005; 127(11): 3801–6.  
[PubMed Abstract](#) | [Publisher Full Text](#)
75. Bates M, Blosser TR, Zhuang X: Short-range spectroscopic ruler based on a single-molecule optical switch. *Phys Rev Lett*. 2005; 94(10): 108101.  
[PubMed Abstract](#) | [Publisher Full Text](#) | [Free Full Text](#)

76. Vogelsang J, Steinbauer C, Forthmann C, et al.: Make them blink: probes for super-resolution microscopy. *Chemphyschem*. 2010; 11(12): 2475–90.  
[PubMed Abstract](#) | [Publisher Full Text](#)
77. Dempsey GT, Vaughan JC, Chen KH, et al.: Evaluation of fluorophores for optimal performance in localization-based super-resolution imaging. *Nat Methods*. 2011; 8(12): 1027–36.  
[PubMed Abstract](#) | [Publisher Full Text](#) | [Free Full Text](#)
78. Shaner NC, Patterson GH, Davidson MW: Advances in fluorescent protein technology. *J Cell Sci.* 2007; 120(Pt 24): 4247–60.  
[PubMed Abstract](#) | [Publisher Full Text](#)
79. Fernández-Suárez M, Ting AY: Fluorescent probes for super-resolution imaging in living cells. *Nat Rev Mol Cell Biol.* 2008; 9(12): 929–43.  
[PubMed Abstract](#) | [Publisher Full Text](#)
80. Wang S, Moffitt JR, Dempsey GT, et al.: Characterization and development of photoactivatable fluorescent proteins for single-molecule-based superresolution imaging. *Proc Natl Acad Sci U S A.* 2014; 111(23): 8452–7.  
[PubMed Abstract](#) | [Publisher Full Text](#) | [Free Full Text](#) | [F1000 Recommendation](#)
81. Huang B, Wang W, Bates M, et al.: Three-dimensional super-resolution imaging by stochastic optical reconstruction microscopy. *Science.* 2008; 319(5864): 810–3.  
[PubMed Abstract](#) | [Publisher Full Text](#) | [Free Full Text](#) | [F1000 Recommendation](#)
82. Jones SA, Shim SH, He J, et al.: Fast, three-dimensional super-resolution imaging of live cells. *Nat Methods.* 2011; 8(6): 499–508.  
[PubMed Abstract](#) | [Publisher Full Text](#) | [Free Full Text](#)
83. Huang B, Jones SA, Brandenburg B, et al.: Whole-cell 3D STORM reveals interactions between cellular structures with nanometer-scale resolution. *Nat Methods.* 2008; 5(12): 1047–52.  
[PubMed Abstract](#) | [Publisher Full Text](#) | [Free Full Text](#)
84. Huang B, Babcock H, Zhuang X: Breaking the diffraction barrier: super-resolution imaging of cells. *Cell.* 2010; 143(7): 1047–58.  
[PubMed Abstract](#) | [Publisher Full Text](#) | [Free Full Text](#)
85. Bates M, Huang B, Dempsey GT, et al.: Multicolor super-resolution imaging with photo-switchable fluorescent probes. *Science.* 2007; 317(5845): 1749–53.  
[PubMed Abstract](#) | [Publisher Full Text](#) | [Free Full Text](#) | [F1000 Recommendation](#)
86. Xu K, Babcock HP, Zhuang X: Dual-objective STORM reveals three-dimensional filament organization in the actin cytoskeleton. *Nat Methods.* 2012; 9(2): 185–8.  
[PubMed Abstract](#) | [Publisher Full Text](#) | [Free Full Text](#) | [F1000 Recommendation](#)
87. Xu K, Zhong G, Zhuang X: Actin, spectrin, and associated proteins form a periodic cytoskeletal structure in axons. *Science.* 2013; 339(6118): 452–6.  
[PubMed Abstract](#) | [Publisher Full Text](#) | [Free Full Text](#) | [F1000 Recommendation](#)
88. Shroff H, Galbraith CG, Galbraith JA, et al.: Dual-color superresolution imaging of genetically expressed probes within individual adhesion complexes. *Proc Natl Acad Sci U S A.* 2007; 104(51): 20308–13.  
[PubMed Abstract](#) | [Publisher Full Text](#) | [Free Full Text](#) | [F1000 Recommendation](#)
89. Kanchanawong P, Shtengel G, Pasapera AM, et al.: Nanoscale architecture of integrin-based cell adhesions. *Nature.* 2010; 468(7323): 580–4.  
[PubMed Abstract](#) | [Publisher Full Text](#) | [Free Full Text](#) | [F1000 Recommendation](#)
90. Annibale P, Vanni S, Scarselli M, et al.: Identification of clustering artifacts in photoactivated localization microscopy. *Nat Methods.* 2011; 8(7): 527–8.  
[PubMed Abstract](#) | [Publisher Full Text](#)
91. Durisic N, Laparra-Cuervo L, Sandoval-Álvarez A, et al.: Single-molecule evaluation of fluorescent protein photoactivation efficiency using an *in vivo* nanotemplate. *Nat Methods.* 2014; 11(2): 156–62.  
[PubMed Abstract](#) | [Publisher Full Text](#)
92. Sengupta P, Jovanovic-Talisman T, Skoko D, et al.: Probing protein heterogeneity in the plasma membrane using PALM and pair correlation analysis. *Nat Methods.* 2011; 8(11): 969–75.  
[PubMed Abstract](#) | [Publisher Full Text](#) | [Free Full Text](#) | [F1000 Recommendation](#)
93. Williamson DJ, Owen DM, Rossy J, et al.: Pre-existing clusters of the adaptor Lat do not participate in early T cell signaling events. *Nat Immunol.* 2011; 12(7): 655–62.  
[PubMed Abstract](#) | [Publisher Full Text](#) | [F1000 Recommendation](#)
94. Rossy J, Owen DM, Williamson DJ, et al.: Conformational states of the kinase Lck regulate clustering in early T cell signaling. *Nat Immunol.* 2013; 14(1): 82–9.  
[PubMed Abstract](#) | [Publisher Full Text](#) | [F1000 Recommendation](#)
95. Steinbauer C, Forthmann C, Vogelsang J, et al.: Superresolution microscopy on the basis of engineered dark states. *J Am Chem Soc.* 2008; 130(50): 16840–1.  
[PubMed Abstract](#) | [Publisher Full Text](#)
96. Lidek K, Rieger B, Jovin T, et al.: Superresolution by localization of quantum dots using blinking statistics. *Opt Express.* 2005; 13(18): 7052–62.  
[PubMed Abstract](#) | [Publisher Full Text](#)
97. Sharonov A, Hochstrasser RM: Wide-field subdiffraction imaging by accumulated binding of diffusing probes. *Proc Natl Acad Sci U S A.* 2006; 103(50): 18911–6.  
[PubMed Abstract](#) | [Publisher Full Text](#) | [Free Full Text](#)
98. Giannone G, Hosy E, Levet F, et al.: Dynamic superresolution imaging of endogenous proteins on living cells at ultra-high density. *Biophys J.* 2010; 99(4): 1303–10.  
[PubMed Abstract](#) | [Publisher Full Text](#) | [Free Full Text](#) | [F1000 Recommendation](#)
99. Schoen I, Ries J, Klotzsch E, et al.: Binding-activated localization microscopy of DNA structures. *Nano Lett.* 2011; 11(9): 4008–11.  
[PubMed Abstract](#) | [Publisher Full Text](#)
100. de Bakker BI, Bodnár A, van Dijk EM, et al.: Nanometer-scale organization of the alpha subunits of the receptors for IL2 and IL15 in human T lymphoma cells. *J Cell Sci.* 2008; 121(Pt 5): 627–33.  
[PubMed Abstract](#) | [Publisher Full Text](#)
101. van Zanten TS, Gómez J, Manzo C, et al.: Direct mapping of nanoscale compositional connectivity on intact cell membranes. *Proc Natl Acad Sci U S A.* 2010; 107(35): 15437–42.  
[PubMed Abstract](#) | [Publisher Full Text](#) | [Free Full Text](#)
102. Zhong L, Zeng G, Lu X, et al.: NSOM/QD-based direct visualization of CD3-induced and CD28-enhanced nanospotential coclustering of TCR and coreceptor in nanodomains in T cell activation. *PLoS One.* 2009; 4(6): e5945.  
[PubMed Abstract](#) | [Publisher Full Text](#) | [Free Full Text](#)
103. Chen Y, Qin J, Chen ZW: Fluorescence-topographic NSOM directly visualizes peak-valley polarities of GM1/GM3 rafts in cell membrane fluctuations. *J Lipid Res.* 2008; 49(10): 2268–75.  
[PubMed Abstract](#) | [Publisher Full Text](#) | [Free Full Text](#)
104. Ianoul A, Grant DD, Rouleau Y, et al.: Imaging nanometer domains of beta-adrenergic receptor complexes on the surface of cardiac myocytes. *Nat Chem Biol.* 2005; 1(4): 196–202.  
[PubMed Abstract](#) | [Publisher Full Text](#)
105. van Zanten TS, Cambi A, Koopman M, et al.: Hotspots of GPI-anchored proteins and integrin nanoclusters function as nucleation sites for cell adhesion. *Proc Natl Acad Sci U S A.* 2009; 106(44): 18557–62.  
[PubMed Abstract](#) | [Publisher Full Text](#) | [Free Full Text](#)
106. Höppener C, Novotny L: Antenna-based optical imaging of single Ca<sup>2+</sup> transmembrane proteins in liquids. *Nano Lett.* 2008; 8(2): 642–6.  
[PubMed Abstract](#) | [Publisher Full Text](#)
107. van Zanten TS, Lopez-Bosque MJ, Garcia-Parajo MF: Imaging individual proteins and nanodomains on intact cell membranes with a probe-based optical antenna. *Small.* 2010; 6(2): 270–5.  
[PubMed Abstract](#) | [Publisher Full Text](#)
108. Mivelle M, van Zanten TS, Garcia-Parajo MF: Hybrid photonic antennas for subnanometer multicolor localization and nanoimaging of single molecules. *Nano Lett.* 2014; 14(8): 4895–900.  
[PubMed Abstract](#) | [Publisher Full Text](#)
109. Garcia-Parajo MF: Optical antennas focus in on biology. *Nat Photonics.* 2008; 2(4): 201–3.  
[Publisher Full Text](#)
110. Hell SW, Wichmann J: Breaking the diffraction resolution limit by stimulated emission: stimulated-emission-depletion fluorescence microscopy. *Opt Lett.* 1994; 19(11): 780–2.  
[PubMed Abstract](#) | [Publisher Full Text](#)
111. Hell SW: Far-field optical nanoscopy. *Science.* 2007; 316(5828): 1153–8.  
[PubMed Abstract](#) | [Publisher Full Text](#)
112. Eggeling C, Willig KI, Sahl SJ, et al.: Lens-based fluorescence nanoscopy. *Q Rev Biophys.* 2015; 48(2): 178–243.  
[PubMed Abstract](#) | [Publisher Full Text](#)
113. Sieber JJ, Willig KI, Kutzner C, et al.: Anatomy and dynamics of a supramolecular membrane protein cluster. *Science.* 2007; 317(5841): 1072–6.  
[PubMed Abstract](#) | [Publisher Full Text](#) | [F1000 Recommendation](#)
114. Kellner RR, Baier CJ, Willig KI, et al.: Nanoscale organization of nicotinic acetylcholine receptors revealed by stimulated emission depletion microscopy. *Neuroscience.* 2007; 144(1): 135–43.  
[PubMed Abstract](#) | [Publisher Full Text](#)
115. Manzo C, van Zanten TS, Saha S, et al.: PSF decomposition of nanoscopy images via Bayesian analysis unravels distinct molecular organization of the cell membrane. *Sci Rep.* 2014; 4: 4354.  
[PubMed Abstract](#) | [Publisher Full Text](#) | [Free Full Text](#)
116. Saka SK, Honigmann A, Eggeling C, et al.: Multi-protein assemblies underlie the mesoscale organization of the plasma membrane. *Nat Commun.* 2014; 5: 4509.  
[PubMed Abstract](#) | [Publisher Full Text](#) | [Free Full Text](#) | [F1000 Recommendation](#)
117. Bingen P, Reuss M, Engelhardt J, et al.: Parallelized STED fluorescence nanoscopy. *Opt Express.* 2011; 19(24): 23716–26.  
[PubMed Abstract](#) | [Publisher Full Text](#)
118. Chmyrov A, Keller J, Grotjohann T, et al.: Nanoscopy with more than 100,000 ‘doughnuts’. *Nat Methods.* 2013; 10(8): 737–40.  
[PubMed Abstract](#) | [Publisher Full Text](#)
119. Donnert G, Keller J, Wurm CA, et al.: Two-color far-field fluorescence nanoscopy. *Biophys J.* 2007; 92(8): L67–9.  
[PubMed Abstract](#) | [Publisher Full Text](#) | [Free Full Text](#) | [F1000 Recommendation](#)
120. Bücker J, Wildanger D, Vicidomini G, et al.: Simultaneous multi-lifetime multi-color STED imaging for colocalization analyses. *Opt Express.* 2011; 19(4): 3130–43.  
[PubMed Abstract](#) | [Publisher Full Text](#)
121. Bergermann F, Alber L, Sahl SJ, et al.: 2000-fold parallelized dual-color STED fluorescence nanoscopy. *Opt Express.* 2015; 23(1): 211–3.  
[PubMed Abstract](#) | [Publisher Full Text](#)
122. Vicidomini G, Moneron G, Han KY, et al.: Sharper low-power STED nanoscopy by

- time gating. *Nat Methods*. 2011; 8(7): 571–3.  
[PubMed Abstract](#) | [Publisher Full Text](#)
123. Staudt T, Engler A, Rittweger E, et al.: Far-field optical nanoscopy with reduced number of state transition cycles. *Opt Express*. 2011; 19(6): 5644–57.  
[PubMed Abstract](#) | [Publisher Full Text](#)
124. He HT, Marguet D: Detecting nanodomains in living cell membrane by fluorescence correlation spectroscopy. *Annu Rev Phys Chem*. 2011; 62(1): 417–36.  
[PubMed Abstract](#) | [Publisher Full Text](#)
125. Wawrzynieck L, Rigneault H, Marguet D, et al.: Fluorescence correlation spectroscopy diffusion laws to probe the submicron cell membrane organization. *Biophys J*. 2005; 89(6): 4029–42.  
[PubMed Abstract](#) | [Publisher Full Text](#) | [Free Full Text](#)
126. Lenne PF, Wawrzynieck L, Conchonaud F, et al.: Dynamic molecular confinement in the plasma membrane by microdomains and the cytoskeleton meshwork. *EMBO J*. 2006; 25(14): 3245–56.  
[PubMed Abstract](#) | [Publisher Full Text](#) | [Free Full Text](#) | [F1000 Recommendation](#)
127. Lasserre R, Guo XJ, Conchonaud F, et al.: Raft nanodomains contribute to Akt/PKB plasma membrane recruitment and activation. *Nat Chem Biol*. 2008; 4(9): 538–47.  
[PubMed Abstract](#) | [Publisher Full Text](#) | [F1000 Recommendation](#)
128. Eggeling C, Hilbert M, Bock H, et al.: Reversible photoswitching enables single-molecule fluorescence fluctuation spectroscopy at high molecular concentration. *Microsc Res Tech*. 2007; 70(12): 1003–9.  
[PubMed Abstract](#) | [Publisher Full Text](#)
129. Vobornik D, Banks DS, Lu Z, et al.: Fluorescence correlation spectroscopy with sub-diffraction-limited resolution using near-field optical probes. *Appl Phys Lett*. 2008; 93(16): 163904.  
[Publisher Full Text](#)
130. Eggeling C, Ringemann C, Medda R, et al.: Direct observation of the nanoscale dynamics of membrane lipids in a living cell. *Nature*. 2009; 457(7233): 1159–62.  
[PubMed Abstract](#) | [Publisher Full Text](#) | [F1000 Recommendation](#)
131. Hermann M, Neuberth N, Wissler J, et al.: Near-field optical study of protein transport kinetics at a single nuclear pore. *Nano Lett*. 2009; 9(9): 3330–6.  
[PubMed Abstract](#) | [Publisher Full Text](#)
132. Manzo C, van Zanten TS, Garcia-Parajo MF: Nanoscale fluorescence correlation spectroscopy on intact living cell membranes with NSOM probes. *Biophys J*. 2011; 100(2): L8–10.  
[PubMed Abstract](#) | [Publisher Full Text](#) | [Free Full Text](#)
133. Ruprecht V, Wieser S, Marguet D, et al.: Spot variation fluorescence correlation spectroscopy allows for superresolution chronoscopy of confinement times in membranes. *Biophys J*. 2011; 100(11): 2839–45.  
[PubMed Abstract](#) | [Publisher Full Text](#) | [Free Full Text](#)
134. Wenger J, Conchonaud F, Dintinger J, et al.: Diffusion analysis within single nanometric apertures reveals the ultrafine cell membrane organization. *Biophys J*. 2007; 92(3): 913–9.  
[PubMed Abstract](#) | [Publisher Full Text](#) | [Free Full Text](#) | [F1000 Recommendation](#)
135. Andrade DM, Clausen MP, Keller J, et al.: Cortical actin networks induce spatio-temporal confinement of phospholipids in the plasma membrane—a minimally invasive investigation by STED-FCS. *Sci Rep*. 2015; 5: 11454.  
[PubMed Abstract](#) | [Publisher Full Text](#) | [Free Full Text](#)
136. Mueller V, Ringemann C, Honigmann A, et al.: STED nanoscopy reveals molecular details of cholesterol- and cytoskeleton-modulated lipid interactions in living cells. *Biophys J*. 2011; 101(7): 1651–60.  
[PubMed Abstract](#) | [Publisher Full Text](#) | [Free Full Text](#)
137. Sezgin E, Levental I, Grzybek M, et al.: Partitioning, diffusion, and ligand binding of raft lipid analogs in model and cellular plasma membranes. *Biochim Biophys Acta*. 2012; 1818(7): 1777–84.  
[PubMed Abstract](#) | [Publisher Full Text](#)
138. Mueller V, Honigmann A, Ringemann C, et al.: FCS in STED microscopy: studying the nanoscale of lipid membrane dynamics. *Method Enzymol*. 2013; 519: 1–38.  
[PubMed Abstract](#) | [Publisher Full Text](#)
139. Honigmann A, Mueller V, Ta H, et al.: Scanning STED-FCS reveals spatiotemporal heterogeneity of lipid interaction in the plasma membrane of living cells. *Nat Commun*. 2014; 5: 5412.  
[PubMed Abstract](#) | [Publisher Full Text](#)
140. Kannan B, Guo L, Sudhaharan T, et al.: Spatially resolved total internal reflection fluorescence correlation microscopy using an electron multiplying charge-coupled device camera. *Anal Chem*. 2007; 79(12): 4463–70.  
[PubMed Abstract](#) | [Publisher Full Text](#)
141. Sankaran J, Bag N, Kraut RS, et al.: Accuracy and precision in camera-based fluorescence correlation spectroscopy measurements. *Anal Chem*. 2013; 85(8): 3948–54.  
[PubMed Abstract](#) | [Publisher Full Text](#)
142. Huang H, Simsek MF, Jin W, et al.: Effect of receptor dimerization on membrane lipid raft structure continuously quantified on single cells by camera based fluorescence correlation spectroscopy. *PLoS One*. 2015; 10(3): e0121777–18.  
[PubMed Abstract](#) | [Publisher Full Text](#) | [Free Full Text](#)
143. Hebert B, Costantino S, Wiseman PW: Spatiotemporal image correlation spectroscopy (STICS) theory, verification, and application to protein velocity mapping in living CHO cells. *Biophys J*. 2005; 88(5): 3601–14.  
[PubMed Abstract](#) | [Publisher Full Text](#) | [Free Full Text](#)
144. Brown CM, Hebert B, Kolin DL, et al.: Probing the integrin-actin linkage using high-resolution protein velocity mapping. *J Cell Sci*. 2006; 119(Pt 24): 5204–14.  
[PubMed Abstract](#) | [Publisher Full Text](#) | [F1000 Recommendation](#)
145. Di Renzo C, Gratton E, Beltram F, et al.: Fast spatiotemporal correlation spectroscopy to determine protein lateral diffusion laws in live cell membranes. *Proc Natl Acad Sci U S A*. 2013; 110(30): 12307–12.  
[PubMed Abstract](#) | [Publisher Full Text](#) | [Free Full Text](#)
146. Abu-Arish A, Pandzic E, Goepf J, et al.: Cholesterol modulates CFTR confinement in the plasma membrane of primary epithelial cells. *Biophys J*. 2015; 109(1): 85–94.  
[PubMed Abstract](#) | [Publisher Full Text](#) | [Free Full Text](#)
147. Moran-Mirabal JM, Torres AJ, Samiee KT, et al.: Cell investigation of nanostructures: zero-mode waveguides for plasma membrane studies with single molecule resolution. *Nanotechnology*. 2007; 18(19): 195101.  
[Publisher Full Text](#)
148. Richards CI, Luong K, Srinivasan R, et al.: Live-cell imaging of single receptor composition using zero-mode waveguide nanostructures. *Nano Lett*. 2012; 12(7): 3690–4.  
[PubMed Abstract](#) | [Publisher Full Text](#) | [Free Full Text](#)
149. Kelly CV, Baird BA, Craighead HG: An array of planar apertures for near-field fluorescence correlation spectroscopy. *Biophys J*. 2011; 100(7): L34–6.  
[PubMed Abstract](#) | [Publisher Full Text](#) | [Free Full Text](#)
150. Kelly CV, Wakefield DL, Holowka DA, et al.: Near-field fluorescence cross-correlation spectroscopy on planar membranes. *ACS Nano*. 2014; 8(7): 7392–404.  
[PubMed Abstract](#) | [Publisher Full Text](#) | [Free Full Text](#) | [F1000 Recommendation](#)
151. Lohmüller T, Iversen L, Schmidt M, et al.: Single molecule tracking on supported membranes with arrays of optical nanoantennas. *Nano Lett*. 2012; 12(3): 1717–21.  
[PubMed Abstract](#) | [Publisher Full Text](#) | [Free Full Text](#)
152. Flauraud V, van Zanten TS, Miville M, et al.: Large-Scale Arrays of Bowtie Nanoaperture Antennas for Nanoscale Dynamics in Living Cell Membranes. *Nano Lett*. 2015; 15(6): 4176–82.  
[PubMed Abstract](#) | [Publisher Full Text](#)
153. Schwille P, Meyer-Almes FJ, Rigler R: Dual-color fluorescence cross-correlation spectroscopy for multicomponent diffusional analysis in solution. *Biophys J*. 1997; 72(4): 1878–86.  
[PubMed Abstract](#) | [Publisher Full Text](#) | [Free Full Text](#)
154. Larson DR, Gosse JA, Holowka DA, et al.: Temporally resolved interactions between antigen-stimulated IgE receptors and Lyn kinase on living cells. *J Cell Biol*. 2005; 171(3): 527–36.  
[PubMed Abstract](#) | [Publisher Full Text](#) | [Free Full Text](#)
155. Triffo SB, Huang HH, Smith AW, et al.: Monitoring lipid anchor organization in cell membranes by PIE-FCCS. *J Am Chem Soc*. 2012; 134(26): 10833–42.  
[PubMed Abstract](#) | [Publisher Full Text](#) | [Free Full Text](#) | [F1000 Recommendation](#)
156. Lee IH, Saha S, Polley A, et al.: Live cell plasma membranes do not exhibit a miscibility phase transition over a wide range of temperatures. *J Phys Chem B*. 2015; 119(12): 4450–9.  
[PubMed Abstract](#) | [Publisher Full Text](#)
157. Suzuki KG, Fujiwara TK, Edidin M, et al.: Dynamic recruitment of phospholipase C gamma at transiently immobilized GPI-anchored receptor clusters induces IP<sub>3</sub>-Ca<sup>2+</sup> signaling: single-molecule tracking study 2. *J Cell Biol*. 2007; 177(4): 731–42.  
[PubMed Abstract](#) | [Publisher Full Text](#) | [Free Full Text](#) | [F1000 Recommendation](#)
158. Weidemann T, Schwille P: Dual-color fluorescence cross-correlation spectroscopy with continuous laser excitation in a confocal setup. *Methods Enzymol*. 2013; 518: 43–70.  
[PubMed Abstract](#) | [Publisher Full Text](#)
159. de Almeida RF, Loura LM, Prieto M: Membrane lipid domains and rafts: current applications of fluorescence lifetime spectroscopy and imaging. *Chem Phys Lipids*. 2009; 157(2): 61–77.  
[PubMed Abstract](#) | [Publisher Full Text](#)
160. Bader AN, Hoetzl S, Hofman EG, et al.: Homo-FRET imaging as a tool to quantify protein and lipid clustering. *Chemphyschem*. 2010; 12(3): 475–83.  
[PubMed Abstract](#) | [Publisher Full Text](#)
161. Sun Y, Wallrabe H, Seo SA, et al.: FRET microscopy in 2010: the legacy of Theodor Förster on the 100th anniversary of his birth. *Chemphyschem*. 2011; 12(3): 462–74.  
[PubMed Abstract](#) | [Publisher Full Text](#) | [Free Full Text](#)
162. Rao M, Mayor S: Use of Förster's resonance energy transfer microscopy to study lipid rafts. *Biochim Biophys Acta*. 2005; 1746(3): 221–33.  
[PubMed Abstract](#) | [Publisher Full Text](#)
163. Varma R, Mayor S: GPI-anchored proteins are organized in submicron domains at the cell surface. *Nature*. 1998; 394(6695): 798–801.  
[PubMed Abstract](#) | [Publisher Full Text](#)
164. Sharma P, Varma R, Saraiji RC, et al.: Nanoscale organization of multiple GPI-anchored proteins in living cell membranes. *Cell*. 2004; 116(4): 577–89.  
[PubMed Abstract](#) | [Publisher Full Text](#) | [F1000 Recommendation](#)
165. Goswami D, Gowrisankar K, Bilgrami S, et al.: Nanoclusters of GPI-anchored proteins are formed by cortical actin-driven activity. *Cell*. 2008; 135(6): 1085–97.  
[PubMed Abstract](#) | [Publisher Full Text](#)

166. Gowrishankar K, Ghosh S, Saha S, et al.: Active remodeling of cortical actin regulates spatiotemporal organization of cell surface molecules. *Cell*. 2012; 149(6): 1353–67.  
[PubMed Abstract](#) | [Publisher Full Text](#) | [F1000 Recommendation](#)
167. Raghupathy R, Anilkumar AA, Polley A, et al.: Transbilayer lipid interactions mediate nanoclustering of lipid-anchored proteins. *Cell*. 2015; 161(3): 581–94.  
[PubMed Abstract](#) | [Publisher Full Text](#) | [Free Full Text](#) | [F1000 Recommendation](#)
168. Tian T, Harding A, Inder K, et al.: Plasma membrane nanoswitches generate high-fidelity Ras signal transduction. *Nat Cell Biol*. 2007; 9(8): 905–14.  
[PubMed Abstract](#) | [Publisher Full Text](#)
169. Iyengar G, Rao M: A cellular solution to an information-processing problem. *Proc Natl Acad Sci U S A*. 2014; 111(34): 12402–7.  
[PubMed Abstract](#) | [Publisher Full Text](#) | [Free Full Text](#)
170. DeMali KA, Wennerberg K, Burridge K: Integrin signaling to the actin cytoskeleton. *Curr Opin Cell Biol*. 2003; 15(5): 572–82.  
[PubMed Abstract](#) | [Publisher Full Text](#)
171. Brakebusch C, Fässler R: The integrin-actin connection, an eternal love affair. *EMBO J*. 2003; 22(10): 2324–33.  
[PubMed Abstract](#) | [Publisher Full Text](#) | [Free Full Text](#)
172. Cotton M, Claing A: G protein-coupled receptors stimulation and the control of cell migration. *Cell Signal*. 2009; 21(7): 1045–53.  
[PubMed Abstract](#) | [Publisher Full Text](#)
173. Choudhuri K, Dustin ML: Signaling microdomains in T cells. *FEBS Lett*. 2010; 584(24): 4823–31.  
[PubMed Abstract](#) | [Publisher Full Text](#) | [Free Full Text](#)
174. Fooksman DR, Vardhana S, Vasiliver-Shamis G, et al.: Functional anatomy of T cell activation and synapse formation. *Annu Rev Immunol*. 2010; 28(1): 79–105.  
[PubMed Abstract](#) | [Publisher Full Text](#) | [Free Full Text](#)
175. Gulyani A, Vitriol E, Allen R, et al.: A biosensor generated via high-throughput screening quantifies cell edge Src dynamics. *Nat Chem Biol*. 2011; 7(7): 437–44.  
[PubMed Abstract](#) | [Publisher Full Text](#) | [Free Full Text](#)
176. Ouyang M, Sun J, Chien S, et al.: Determination of hierarchical relationship of Src and Rac at subcellular locations with FRET biosensors. *Proc Natl Acad Sci U S A*. 2008; 105(38): 14353–8.  
[PubMed Abstract](#) | [Publisher Full Text](#) | [Free Full Text](#)
177. Seong J, Ouyang M, Kim T, et al.: Detection of focal adhesion kinase activation at membrane microdomains by fluorescence resonance energy transfer. *Nat Commun*. 2011; 2: 406–9.  
[PubMed Abstract](#) | [Publisher Full Text](#) | [Free Full Text](#) | [F1000 Recommendation](#)
178. Hinde E, Dignan MA, Hahn KM, et al.: Millisecond spatiotemporal dynamics of FRET biosensors by the pair correlation function and the phasor approach to FLIM. *Proc Natl Acad Sci U S A*. 2013; 110(1): 135–40.  
[PubMed Abstract](#) | [Publisher Full Text](#) | [Free Full Text](#) | [F1000 Recommendation](#)
179. Manz BN, Jackson BL, Petit RS, et al.: T-cell triggering thresholds are modulated by the number of antigen within individual T-cell receptor clusters. *Proc Natl Acad Sci U S A*. 2011; 108(22): 9089–94.  
[PubMed Abstract](#) | [Publisher Full Text](#) | [Free Full Text](#) | [F1000 Recommendation](#)
180. Schwarzenbacher M, Kaltenbrunner M, Brameshuber M, et al.: Micropatterning for quantitative analysis of protein-protein interactions in living cells. *Nat Methods*. 2008; 5(12): 1053–60.  
[PubMed Abstract](#) | [Publisher Full Text](#) | [F1000 Recommendation](#)
181. Sevcik E, Brameshuber M, Fölscher M, et al.: GPI-anchored proteins do not reside in ordered domains in the live cell plasma membrane. *Nat Commun*. 2015; 6: 6969.  
[PubMed Abstract](#) | [Publisher Full Text](#) | [Free Full Text](#)
182. Salaita K, Nair PM, Petit RS, et al.: Restriction of receptor movement alters cellular response: physical force sensing by EphA2. *Science*. 2010; 327(5971): 1380–5.  
[PubMed Abstract](#) | [Publisher Full Text](#) | [Free Full Text](#) | [F1000 Recommendation](#)
183. Caculian NG, Kai H, Liu EY, et al.: Size-based chromatography of signaling clusters in a living cell membrane. *Nano Lett*. 2014; 14(5): 2293–8.  
[PubMed Abstract](#) | [Publisher Full Text](#) | [Free Full Text](#)
184. Levskaya A, Weiner OD, Lim WA, et al.: Spatiotemporal control of cell signalling using a light-switchable protein interaction. *Nature*. 2009; 461(7266): 997–1001.  
[PubMed Abstract](#) | [Publisher Full Text](#) | [Free Full Text](#) | [F1000 Recommendation](#)
185. Zhou XX, Chung HK, Lam AJ, et al.: Optical control of protein activity by fluorescent protein domains. *Science*. 2012; 338(6108): 810–4.  
[PubMed Abstract](#) | [Publisher Full Text](#) | [Free Full Text](#) | [F1000 Recommendation](#)
186. Strickland D, Lin Y, Wagner E, et al.: TULIPs: tunable, light-controlled interacting protein tags for cell biology. *Nat Methods*. 2012; 9(4): 379–84.  
[PubMed Abstract](#) | [Publisher Full Text](#) | [Free Full Text](#) | [F1000 Recommendation](#)
187. Kawano F, Suzuki H, Furuya A, et al.: Engineered pairs of distinct photoswitches for optogenetic control of cellular proteins. *Nat Commun*. 2015; 6: 6256.  
[PubMed Abstract](#) | [Publisher Full Text](#) | [F1000 Recommendation](#)
188. Loose M, Fischer-Friedrich E, Ries J, et al.: Spatial regulators for bacterial cell division self-organize into surface waves *in vitro*. *Science*. 2008; 320(5877): 789–92.  
[PubMed Abstract](#) | [Publisher Full Text](#) | [F1000 Recommendation](#)
189. Iversen L, Tu HL, Lin WC, et al.: Molecular kinetics. Ras activation by SOS: allosteric regulation by altered fluctuation dynamics. *Science*. 2014; 345(6192): 50–4.  
[PubMed Abstract](#) | [Publisher Full Text](#) | [Free Full Text](#) | [F1000 Recommendation](#)
190. Honigmann A, Sadeghi S, Keller J, et al.: A lipid bound actin meshwork organizes liquid phase separation in model membranes. *eLife*. 2014; 3: e01671.  
[PubMed Abstract](#) | [Publisher Full Text](#) | [Free Full Text](#) | [F1000 Recommendation](#)
191. Milovanovic D, Honigmann A, Koike S, et al.: Hydrophobic mismatch sorts SNARE proteins into distinct membrane domains. *Nat Commun*. 2015; 6: 5984.  
[PubMed Abstract](#) | [Publisher Full Text](#) | [Free Full Text](#) | [F1000 Recommendation](#)
192. Zieske K, Schwille P: Reconstitution of self-organizing protein gradients as spatial cues in cell-free systems. *eLife*. 2014; 3: e03949.  
[PubMed Abstract](#) | [Publisher Full Text](#) | [Free Full Text](#)
193. Levental I, Grzybek M, Simons K: Raft domains of variable properties and compositions in plasma membrane vesicles. *Proc Natl Acad Sci U S A*. 2011; 108(28): 11411–6.  
[PubMed Abstract](#) | [Publisher Full Text](#) | [Free Full Text](#)
194. Schwille P: Bottom-up synthetic biology: engineering in a tinkerer's world. *Science*. 2011; 333(6047): 1252–4.  
[PubMed Abstract](#) | [Publisher Full Text](#)

## Open Peer Review

Current Referee Status:



### Editorial Note on the Review Process

F1000 Faculty Reviews are commissioned from members of the prestigious F1000 Faculty and are edited as a service to readers. In order to make these reviews as comprehensive and accessible as possible, the referees provide input before publication and only the final, revised version is published. The referees who approved the final version are listed with their names and affiliations but without their reports on earlier versions (any comments will already have been addressed in the published version).

### The referees who approved this article are:

#### Version 1

- 1 Christian Eggeling, Radcliffe Department of Medicine, University of Oxford, Oxford, UK

**Competing Interests:** No competing interests were disclosed.

- 2 Paul W Wiseman, Department of Chemistry, McGill University, Montréal, Quebec, H3A 0B8, Canada

**Competing Interests:** No competing interests were disclosed.

- 3 Mary L Kraft, Department of Chemistry, University of Illinois at Urbana-Champaign, Urbana, IL, USA

**Competing Interests:** No competing interests were disclosed.